Morphological variation in *Blommersia* pelvic shape coincides with muscular architecture and parallels genus phylogenetic evolution

Javier H. Santos-Santos[1,2], Mireia Guinovart-Castán[1], David R. Vieites[1]

[1] *Department of Biogeography and Global Change (BGC-MNCN-CSIC), Museo Nacional de Ciencias Naturales, C/José Gutiérrez Abascal 2, E-28006, Madrid, Spain.*

[2] *Department of Animal Biology, University of Barcelona, Avenida Diagonal 645, 08028, Barcelona, Spain.*

ABSTRACT

Mantellids are a hyperdiverse group of frogs endemic to Madagascar, showing a large variation in morphology and ecological specialization that parallels their phylogenetic diversification. Among them, the genus *Blommersia* comprises several small species of small to miniature frogs, two of which occur in syntopy on the Comorian archipelago, which was colonized by their ancestor several millions of years ago in an event of transoceanic dispersal from Madagascar. They have evolved in isolation, which has supposed an evolutionary experiment of morphological and genetic divergence without competition. In mantellids, as well as in other amphibians, body size is correlated with dispersal capabilities and these may have allowed the colonization of new habitats in parallel to morphological divergence. Consequently, we hypothesized that variation in the *Blommersia* musculoskeletal anatomy implicated in locomotor performance would reflect potential differences between species in accordance to their diversification into different ecological niches and lifestyles. To tackle this question we focused on one of the main components of the anuran locomotor system: the pelvis. We compared the pelvic shape of seven *Blommersia* species, with special emphasis on the Comorian sister species pair and their Malagasy sister taxon. In addition, we mapped for the first time the insertion sites of the musculature on the *Blommersia* pelvis by means of a customized contrast staining technique prior to CT-scanning. Morphological distances resulting from the pelvic shape comparison between species correlated to a high extent with their 16S phylogenetic distances. In accordance, we discuss the observed patterns of pelvic shape variation and their relationship with size variation in the context of pelvic musculoskeletal architecture evolution in anurans and its potential interactions with locomotor function in the *Blommersia* genus.

KEYWORDS: *Blommersia*, computed tomography, contrast staining, musculoskeletal anatomy, pelvic shape.

INTRODUCTION

The role of adaptive radiations as generators of biodiversity is a main topic in evolutionary biology, albeit the mechanisms by which species diversify are still far from being completely understood. Accordingly extensive research has been carried out on the topic aiming to interpret the patterns and processes of speciation. Ecological, environmental, genetic, historical, functional, and reproductive factors have all been evoked to explain diversification in different situations. Even though all of these factors influence different aspects of organismal evolution, most of them have directly or indirectly contributed to shaping species' morphology and aided in their divergence.

Extant anurans are characterized for having a highly-derived musculoskeletal anatomy as a result of evolution to their bimodal lifestyle in both aquatic and terrestrial habitats (Handrigan & Wassersug, 2007; Gillis, 2010). Morphological specializations include a truncated axial skeleton, fused post-sacral vertebrae into an urostyle, elongated iliac shafts that articulate with the sacral diapophyses, fused pubis and ischium with the posterior ilium in a wheel-like acetabular structure, fused zeugopodian elements, and relatively long hindlimbs. Their specialized morphology is a clear reflection of a many-to-one mapping of form to function (Wainwright et al., 2005) in view of the large diversity of locomotor modes they have achieved with minimal changes to their *bauplan* (aka body plan), which has allowed them to colonize about every potential habitat (Duellman & Trueb, 1994). To this respect, there appears to be a strong relationship between the ilio-sacral and sacral-urostylic articulations and preferred locomotor mode in anurans (Emerson, 1982; Reilly & Jorgensen, 2011). The variation in articulation types confers, reduces, or transfers mobility, granting mechanical advantage to specific movements involved in each locomotor mode. For example, specialized long-distance jumpers have repeatedly evolved a sagittal-hinge type ilio-sacral articulation that restricts movement to the vertical (*i.e.* sagittal) plane, and a bicondylar sacro-urostylic joint that provides additional axial rigidity to lateral-bending behaviors. While these structural differences in skeletal elements have proven to largely predict locomotor mode, size differences and/or shape modifications in them can also alter the distribution, size, and properties of associated musculature influencing locomotor performance (Emerson, 1978; Zug, 1978; Emerson & De Jongh, 1980; James et al., 2007).

Jumping locomotion in basal anurans is believed to have evolved in response to escape predators on land, foraging, and/or increase dispersal capabilities (Gans & Parsons, 1966; Prikryl et al., 2009; Essner et al., 2010; Sigurdsen et al., 2012; Lires et al., 2016). Throughout the evolution of the anuran *bauplan*, it is clear from that mentioned beforehand that pelvic morphology has played an important role in their functional diversification and geographic dispersal. Hence, we can expect that the selective pressures that have shaped this morphofunctional structure are still at work in extant species as they adapt to novel environments and different ecological pressures (Gomes et al., 2009; Hudson et al., 2016).

In Madagascar there are five endemic frog radiations with ~100% species endemism, of which the Mantellidae represent the largest adaptive radiation with 214 described species (amphibiaweb.org) and many more yet to be described (Vieites et al., 2009). Within these Malagasy radiations, the degree of morphological variation is large and its impact on species' diversification and distribution patterns of importance, but not yet fully understood. For example, it has been observed that body size influences species' range size and biogeographic setting in Madagascar, potentially influencing dispersal and speciation rates (Wollenberg et al., 2011; Pabijan et al., 2012). These processes are repercussive in species under processes of miniaturization, or nanism (Whittaker et al., 2007), which appears to be the trend in Malagasy mantellids and microhylids (Scherz et al., 2017a; 2017b). In these species, selective pressures have driven a reduction in their anatomy as an adaptive response to different ecological niches, although entailing strong biological constraints in order to maintain organ function at very small sizes. Up-to-date there are no studies concerning the impact of body size evolution on the musculoskeletal system of mantellids nor on its resulting influence on jumping performance, which can relate directly to their habitat selection, dispersal capability, and biogeographic speciation pattern.

The current study constitutes the first comparison within the Mantellidae of a functionally-relevant trait implicated in locomotor performance. We take advantage of a natural evolutionary experiment occurring on the Comorian archipelago, originated 6.5 Mya by the transoceanic dispersal of their most recent common ancestor from mainland Madagascar to Mayotte. This *Blommersia* ancestor diverged in sympatry on the island, producing two genetically-distinct syntopic sister species that differ in morphology and

breeding ecology (Chapter 3). More interestingly, one presents a trend of decreasing body size relative to its closest mainland sister taxon (*B. wittei*), while the other, one of increasing body size (Chapter 3). Given that the muscles implicated in locomotor mode and function insert on the pelvis, we hypothesize that differential adaptations to species' ecological niche will have generated divergent morphological variation in pelvic structure (Duncan & Turner, 1995). In addition, we search for any potential phylogenetic patterns in pelvic morphological variation by comparison between the Comorian sister species and their closest Malagasy relative, and between these and other Malagasy *Blommersia* representatives.

MATERIALS & METHODS

Specimens

A total of 41 frogs pertaining to seven phylogenetically-proximal *Blommersia* species (Table 1) were retrieved from the Vieites' Lab Collection (DRV) to be catalogued at the National Museum of Natural History, Madrid (MNCN-CSIC) and loaned from the herpetological collection of the Department of Animal Biology at the University of Antananarivo (UADBA). Individuals were selected based upon availability and anatomical integrity with the intention of covering the observable range of variation within each species, including male-female proportions and geographical locations. Most individuals were collected recently by the authors (JHS-S and DRV) in fieldwork excursions to Mayotte and Madagascar. Both Comorian sister species, *B. sp1 small* and *B. sp2 big*, are pending formal taxonomic description (Chapter 3), and the complete skeletal description of *B. sp2 big* is pending publication (Chapter 4). Measurements of snout-vent length and hindlimb length were taken on all specimens with a caliper (0.1 mm).

Morphological Data Acquisition

In order to obtain the precise morphology of the pelvic skeleton without the destruction of the museum samples, specimens were fixed with cotton and submerged in 70% ethanol within 50 mL polypropylene falcon tubes before CT-scanning (*i.e.* computed tomography) in a Nikon XT H-160 system [reconstructed voxel size (µm) = 18-38 (isometric); X-ray (kV) = 53-58; X-ray (µA) = 169-188; Projections = 1800; voxels = 1008] at the internal Service of Non-destructive Techniques (MNCN-CSIC). The CT-

scans were reconstructed with CT Pro 3D software and volumes rendered in VGStudio Max 2.2 © (Volume Graphics GmbH, VGL). Isosurfaces were determined through visual examination for each specimen by the same observer (MG-C) to best capture the density histogram of the skeletal structures that constitute the pelvis. Subsequently, bioinformatics segmentation of the pelvis was done manually by separating the head of the femur from the acetabulum and the sacral vertebra from the pelvis at the ilio-sacral articulation. The resulting segmentation was then extracted as a 3D polygon volumetric model (.ply). Polygon models were then post-processed in MeshLab (Cignoni et al., 2008). Computational error/noise in the models' point clouds were corrected as well as any incongruence in their triangulation. In addition, anatomically non-homologous structures (*e.g.* individual-unique bony hypertrophies) were removed from the models to standardize pelvic shape for intra- and inter-specific shape variation comparisons. Lastly, only the external surface of the volumetric model was kept for downstream analyses to further avoid anatomical non-homologies in the bone's internal structure. Final models ranged from 30 – 134k polygons (median = 52k).

To visualize hindlimb musculature and corroborate muscle insertion sites on the surface of the pelvis, additional Comorian specimens of both species were stained prior to CT-scanning to increase the images' contrast between tissue types (Table S1). We followed a custom protocol that is reversible in most part and does not cause damage to the rare samples in order to maintain their potential consultation unaltered for future reference. First samples were washed in running tap water for 8h prior to an initial staining in a 2.5% phosphomolibdic acid solution within a vacuum chamber for one week (Descamps et al., 2014). Later specimens were stained a second time in a 100% IKI [I2 1% ; KI 2%] solution for an additional 24h (Gignac & Kley, 2014). Subsequently excess iodine was washed during 8h and samples were submerged in a phosphate-buffered saline solution for 48h to rehydrate muscle tissues prior to scanning (Vickerton et al., 2013). The staining procedure was carried out at the Evolutionary Morphology of Vertebrates Lab of Ghent University, Belgium and CT-scans were performed with a custom setup [reconstructed voxel size (µm) = 30-35 (isometric); X-ray (kV) = 80; X-ray (µA) = 375; Projections = 1801; voxels = 1166] at the Center for X-ray Tomography (UGCT).

Table 1. Holding collections and field numbers of the *Blommersia* specimens whose pelvis were compared in the current study. Sex is indicated when available. Localities are indicated for Comorian specimens. In addition, average snout-vent length (SVL) and hindlimb length (HL) are given for each species in mm.

Species	Collection	Field no.	Sex	Locality	SVL	HL
B. blommersae (Guibé, 1974)	UADBA	ZCMV8	-	-	18.4 ± 0.9	34.2 ± 1
	UADBA	FG/MV633	-	-		
B. domerguei (Guibé, 1974)	UADBA	ZCMV271	-	-	14.4 ± 0.3	23.7 ± 0.5
	UADBA	ZCMV272	-	-		
B. grandisonae (Guibé, 1974)	UADBA	MV1356	-	-	20.4 ± 0.6	35.7 ± 3.8
	UADBA	ZCMV5491	-	-		
B. sarotra (Glaw & Vences, 2002)	MNCN	DRV8867	M	-	18.6 ± 0.5	33.1 ± 1.9
	MNCN	DRV8870	M	-		
B. sp2 big	MNCN	DRV6805	F	Mont Combani	26.9 ± 2.6	54.1 ± 4.9
	MNCN	DRV6807	M	Mont Sapere		
	MNCN	DRV6813	F	Mont Sapere		
	MNCN	DRV6832	M	Mont Bénara		
	MNCN	DRV6833	M	Mont Bénara		
	MNCN	DRV6835	M	Mont Choungi		
	MNCN	DRV6836	M	Mont Bénara		
	MNCN	DRV6841	M	Mont Bénara		
	MNCN	DRV6848	F	Mont Combani		
	MNCN	DRV6851	F	Mont Combani		
B. sp1 small	MNCN	DRV6808	F	Mont Sapere	20.1 ± 1.6	37.3 ± 2.2
	MNCN	DRV6854	F	Mont Sapere		
	MNCN	DRV6855	F	Mont Sapere		
	MNCN	DRV6857	M	Mont Sapere		
	MNCN	DRV6859	M	Mont Sapere		
	MNCN	DRV6860	M	Mont Sapere		
	MNCN	DRV6862	M	Mont Sapere		
	MNCN	DRV6863	M	Mont Sapere		
	MNCN	DRV6864	M	Mont Sapere		
	MNCN	DRV6866	M	Mont Sapere		
	MNCN	DRV6867	M	Mont Sapere		
	MNCN	DRV6868	F	Mont Sapere		
	MNCN	DRV6869	F	Mont Sapere		
B. wittei (Guibé, 1974)	MNCN	DRV8719	M	-	24.3 ± 1.3	41.1 ± 2.5
	MNCN	DRV8755	M	-		
	MNCN	DRV8767	M	-		
	MNCN	DRV8768	M	-		
	MNCN	DRV8784	F	-		
	MNCN	DRV8816	F	-		
	UADBA	FGZC376	-	-		
	UADBA	FGZC406	-	-		
	UADBA	FGZC1466	-	-		
	UADBA	FGZC3139	-	-		

Morphological Data Analysis

Pelvic shape was compared by means of a novel landmark-less geometric morphometric technique: Generalized Procrustes Surface Analysis (GPSA; Pomidor et al., 2016). This new method allows the exploitation of morphological output resulting from high-resolution scanning technology without the time-consuming process of identification and digitization of functionally homologous landmarks on the structure of interest. GPSA

adapts the Iterative Closest Point algorithms (Besl & McKay, 1992; Chen & Medioni, 1992) to the Generalized Procrustes Analysis paradigm (Rohlf & Slice, 1990) to perform a symmetric superimposition of model surfaces and calculate an associated distance metric, the Procrustes Surface Metric (PSM), analogous to Procrustes distance that quantifies shape difference (Pomidor et al., 2016). For accurate superimposition an individual must be chosen as the prototype in an analysis on the basis that it is the most complete, most representative, and least morphometrically atypical individual in the dataset. Analyses were performed in the Java © executable provided by Pomidor upon personal request and available at http://morphlab.sc.fsu.edu/software/gpsa/index.html. These were performed with and without size standardization (*i.e.* centroid size = 1) to evaluate the influence of size differences between individuals and species in intra- and inter-specific pelvic shape comparisons.

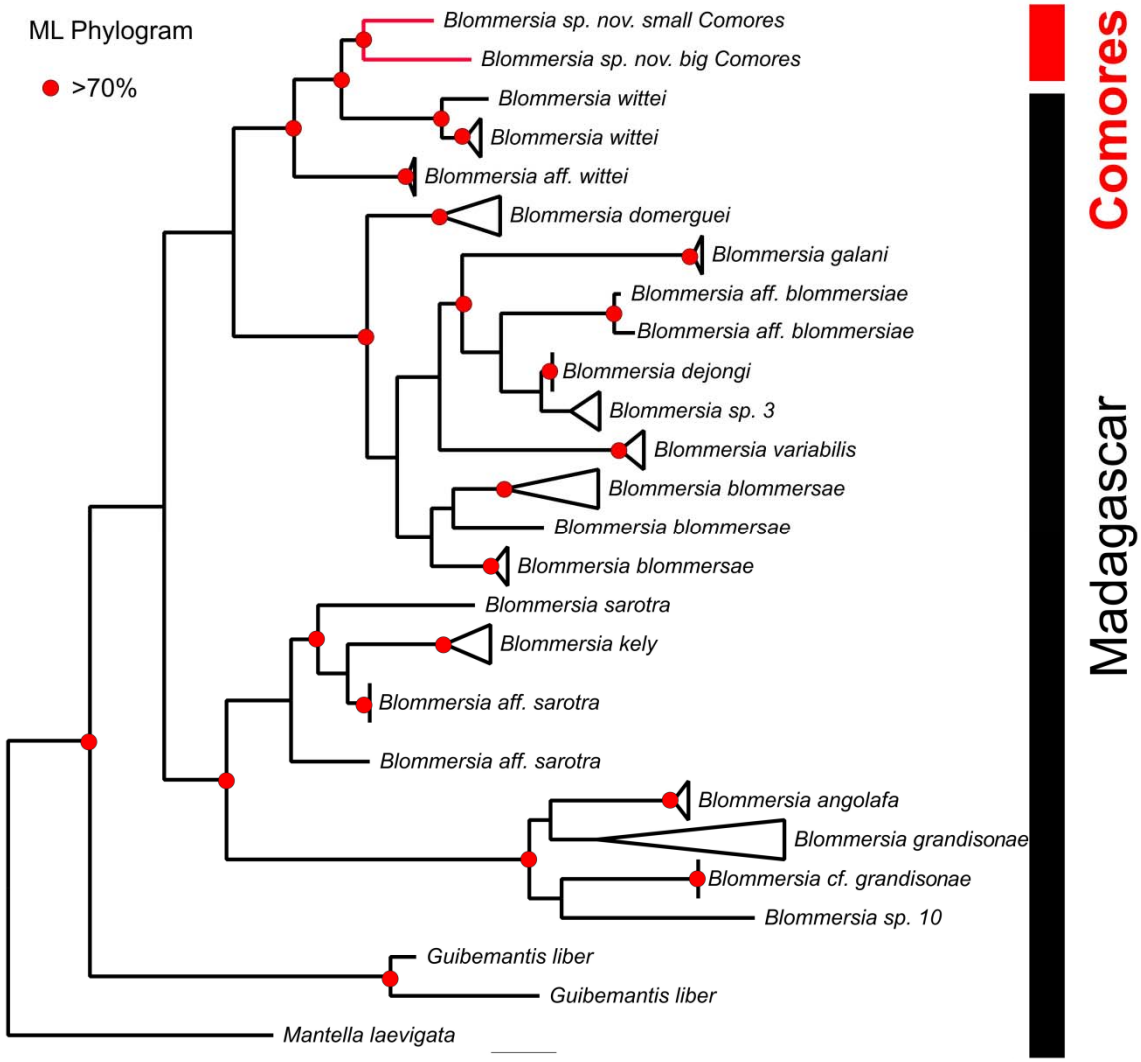

Fig. 1. Maximum Likelihood phylogenetic reconstruction of 16S rRNA relationships within *Blommersia*. Nodes with Maximum Likelihood statistical support higher than 70% are shown in red.

We assessed the intraspecific variation in pelvic morphology through GPSA on datasets of the Comorian sister species and their Malagasy sister taxon, and its interspecific variation on datasets consisting of all possible combinations of these three species. An individual of the *Blommersia wittei* sample was always used as the prototype in analyses containing the three species. In addition, to focalize pelvic shape changes on more potentially biologically-meaningful interspecific variation, we performed interspecific GPSA analyses on a dataset consisting of the mean pelvic shapes for these three species and on another dataset consisting in the mean pelvic shapes of all seven *Blommersia* species. Interspecimen PSM values were compared across analyses, and Principal Coordinate Analysis (PCoA) scores resulting from GPSA pointwise comparisons were plotted in R v3.5.1 statistical software (https://www.R-project.org) to visualize the distribution of specimens along PCoA shape axes. Differences between species in PSM values and PCoA loadings were evaluated statistically in IBM SPSS Statistics v23 (α = 0.05). For each GPSA analysis, overall pelvic shape disparity and the pelvic shape variation explained by each PCoA axes are visualized independently on the sample's mean surface in 3D by means of a color-coded heatmap based on the variation in PSM value at each vertex of the model relative to the sample's consensus.

Phylogenetic Data

Mitochondrial rRNA 16S sequences were compiled from Genbank for all available *Blommersia* species. The same 16S fragment was gathered for the two Comorian species that do not appear in Genbank by the Vieites Lab from a large RNAseq dataset. Sequences were aligned under the Clustal-Wallis algorithm using Genious software, and these were filtered for the same seven species of the morphological analysis (Fig. 1). In order to estimate evolutionary divergence between species a genetic distance matrix was calculated using the Maximum Composite Likelihood model (Tamura et al., 2004). The rate variation among sites was modelled with a gamma distribution (shape parameter = 1). All positions with less than 95% coverage were eliminated, meaning that fewer than 5% alignment gaps, missing data, and ambiguous bases were allowed at any position. There were a total of 475 positions in the final dataset. Analyses were performed in MEGA6 software (Tamura et al., 2013). To determine whether or not there is correlation between observed genetic and morphological variation within the *Blommersia* genus, a Mantel test

(1000 permutations) was performed in R comparing 16S genetic and PSM distance matrices.

Fig. 2. Imprints of the pelvic musculature insertion areas on the 3D pelvic model of the DRV6834 *B. sp2 big* specimen. Insertion areas are not perfectly drawn to scale (see text). Numbers designate the muscles found in Table 2 [m. coccygeoiliacus not drawn]. The hashed area of the m. iliacus internus indicates its position on the medial face of the iliac shaft. The * denotes the relative position of the *Blommersia* femoral gland.

RESULTS

Characterization of Blommersia Pelvic Musculature

CT-scans of stained specimens were examined to locate and identify the different muscles inserting onto the *Blommersia* pelvis. As the representative of our species, and due to its larger size that facilitates visualization, we extracted a 3D model of the pelvis of a *B. sp2 big* specimen (DRV6834) and mapped onto the model's surface its corresponding muscles insertions coming from the stained CT-scan of the same animal (Fig. 2). This procedure allows for a reasonable visualization of the relative positions of

Table 2. Pelvic musculature names, locomotor function, and insertion area based on Duellman & Trueb, 1994 and Prikryl et al., 2009. Muscle numbers match Figure 2.

#	Muscle Complex	Muscle	Locomotor Function	Pelvic Insertion Area
1		**obliquus externus**	Hypaxial flank musculature: provides support for the viscera and exerts a ventral force on the axial column	Lateral anterior ilial shaft
2		**transversus**	Hypaxial flank musculature: provides support for the viscera and exerts a ventral force on the axial column	Ventrolateral surface of the anterior ilial shaft
3		**iliacus externus**	draws the femur forward and flexes the hip joint	Mid-region of the lateral ilial shaft and crest
4	triceps femoris	**glutaeus magnus**	extends the knee joint and flexes the hip joint	Anterolateral region of the posterior ilial process
5		**iliofibularis**	abducts the femur and flexes the knee	Posteroventral region of the posterior ilial process
6		**iliofemoralis**	retraction and adduction of the femur; draws the femur dorsally	Posterodorsal region of the posterior ilial process
7	triceps femoris	**tensor fascia latae**	extends the knee joint and flexes the hip joint	Lateral surface of the ventral mid-region of the ilial shaft
8		**iliacus internus**	protracts and abducts the femur	Lateral and medial posterior ilium base and preacetabulum
9		**coccygeoilicaus**	Epaxial musculature: rotates the urostyle ventrally	Medial surface of the ilial shaft and ilial crest
10		**semimembranosus**	adducts the femur and flexes the knee joint	Dorsoposterior ischium margin
11	obturator externus-gemellus-quadratus femoris	**gemellus**	pulls the femur ventrally	Anterior lateral ischium surface
12	sartoriosemitendinosus	**semitendinosus (dorsal head)**	abducts the femur, pulls the femur ventrally, and flexes the knee joint	Posterior lateral ischium surface
13	gracilis	**gracilis major**	pulls the thigh backwards, flexes the knee joint, and extends the hip joint	Posterior ischium border
14		**adductor magnus (dorsal head)**	adducts the hip joint	Ventral ischium margin
15		**quadratus femoris**	pulls the femur ventrally	Ventrolateral ischium surface
16		**adductor magnus (ventral head)**	adducts the hip joint	Ventral pubic margin
17	sartoriosemitendinosus	**semitendinosus (ventral head)**	abducts the femur, pulls the femur ventrally, and flexes the knee joint	Posteroventral pelvis lateral surface at pubis-ischium union
18	obturator externus-gemellus-quadratus femoris	**obturator externus**	pulls the femur ventrally	Ventral lateral pubic surface
19	sartoriosemitendinosus	**sartorius**	abducts the femur, pulls the femur ventrally, and flexes the knee joint	Anteroventral preacetabular ilium base and pubic margin
20	pectineus-adductor longus	**adductor longus**	adducts and protracts the femur	Anteroventral preacetabular ilium base and pubic lateral surface
21	pectineus-adductor longus	**pectineus**	adducts the femur; fixes the femur in the acetabulum	Pubic lateral surface
22		**obturator internus**	pulls the femur dorsally and rotates the femur	Complete outer acetabulum labrum margin, excluding its most-dorsal margin
23	triceps femoris	**cruralis**	extends the knee joint and flexes the hip joint	Anteroventral margin of the acetabulum

the pelvic musculature; however muscle insertion areas are not perfectly drawn to scale due to differences in the depth along the 2D plane of the volume at which muscles insert. To obtain a more precise characterization of the pelvic musculature, including muscles volumes, and its architecture, a complete segmentation of the *Blommersia* pelvic musculature is underway. For the time being we provide a video of the pelvic musculature across the frog's sagittal plane and several images of the ongoing segmentation in the Supplementary Material.

Table. 3. Morphological disparity for *Blommersia* intra- and inter-specific comparisons of pelvic shape.

Species	Pelvic Morphological Disparity					
	CS = 1					
	min.	max.	range	min.	max.	range
B. sp2 big	0.006 ± 2E-6	0.059 ± 0.003	0.053	0.022 ± 2E-5	0.263 ± 0.05	0.241
B. sp1 small	0.008 ± 6E-6	0.076 ± 0.007	0.068	0.020 ± 2E-5	0.142 ± 0.03	0.122
B. wittei	0.006 ± 2E-6	0.058 ± 0.007	0.052	0.016 ± 2E-5	0.340 ± 0.06	0.323
B. sp2 big - B. sp1 small	0.009 ± 1.2E-5	0.056 ± 0.004	0.047	0.026 ± 1E-4	0.203 ± 0.05	0.177
B. sp2 big - B. wittei	0.009 ± 1E-5	0.116 ± 0.005	0.107	0.029 ± 1E-4	0.358 ± 0.08	0.329
B. sp1 small - B. wittei	0.010 ± 1.6E-5	0.066 ± 0.015	0.056	0.022 ± 6E-5	0.253 ± 0.07	0.231
B. sp2 big - B. sp1 small - B. wittei	0.010 ± 1.5E-5	0.053 ± 0.004	0.043	0.030 ± 1.6E-4	0.327 ± 0.14	0.297
B. sp2 big - B. sp1 small - B. wittei	0.003 ± 3E-9	0.083 ± 0.003	0.080	0.015 ± 1E-8	0.368 ± 0.13	0.353
7 Blommersia spp.	0.011 ± 2.1E-5	0.060 ± 0.020	0.049	0.031 ± 2.4E-4	0.356 ± 0.15	0.325
7 Blommersia spp.	0.006 ± 2E-6	0.079 ± 0.007	0.073	0.023 ± 2E-5	0.339 ± 0.20	0.315

The average minimum, maximum, and range of pointwise variance are given for each comparison. Analyses in bold indicate they were performed on species' mean shape models. Values in the left column correspond to analyses standardized for size, ie. centroid size (CS) = 1.

Pelvic Morphological Disparity

Morphological disparity as reflected by variance at each vertex of the pelvis model in intraspecific pelvic shape is largest in *B. sp1 small*. However, when including size variation in the analyses it is *B. wittei* who presents the highest disparity followed by *B. sp2 big* (Table 3). PSM values of individuals to their respective consensus across intraspecific analyses were not significantly different when standardizing for size (p =

0.487), however there was a significant difference between *B. sp2 big* (0.15) and *B. wittei* (0.07) when including size variation in the analyses ($p = 0.021$).

Pelvic morphological disparity in interspecific comparisons resulted the largest between *B. sp2 big* and *B. wittei*, and the smallest between the Comorian sister species. When including size variation in the analyses the same pattern holds (Table 3). PSM values of individuals to their respective interspecific analysis consensus were not significantly different when standardized for size, however when including size variation in the analyses ($p < 0.05$) *B. sp2 big* presents the largest PSM values and *B. wittei* larger than *B. sp1 small*.

Differences across interspecific comparisons using either individual or species' mean models revealed that larger morphological disparity is observed when utilizing species' mean models (Table 3). As would be expected, all analyses increased in morphological disparity value when including size variation. An ANOVA on individual's centroid size values revealed significant differences between the three species ($F = 39.35$; $p < 0.001$), with *B. sp1 small* presenting the smallest size (2.4) compared to *B. wittei* (2.7) and *B. sp2 big* (3.3). This analysis was not performed on the seven species sample due to insufficient sample size for the remaining species.

Ordination of Pelvic Shape Variation
Intraspecific

PCoA on intraspecific pelvis shape variation displayed significant differences between male and female distribution in shape space only for size-standardized *B. sp1 small* (Wilk's $\lambda = 0$; $p = 0.005$). For this species, females presented significantly lower values on PCo1 ($p = 0.011$; Fig. 3).

Shape variation associated with lower PCo1 values (Fig. 3) consists in an overall decrease in size and robustness of the pelvis. This results in a relatively decreased aperture of the iliac shafts, a relative decrease in height and length of the iliac shafts, a relative decrease in the angle of inclination of the iliac crests, and a relative decrease in robustness of the entire acetabular portion of the pelvis, especially at the iliac process and posterodorsal ilium and ischium.

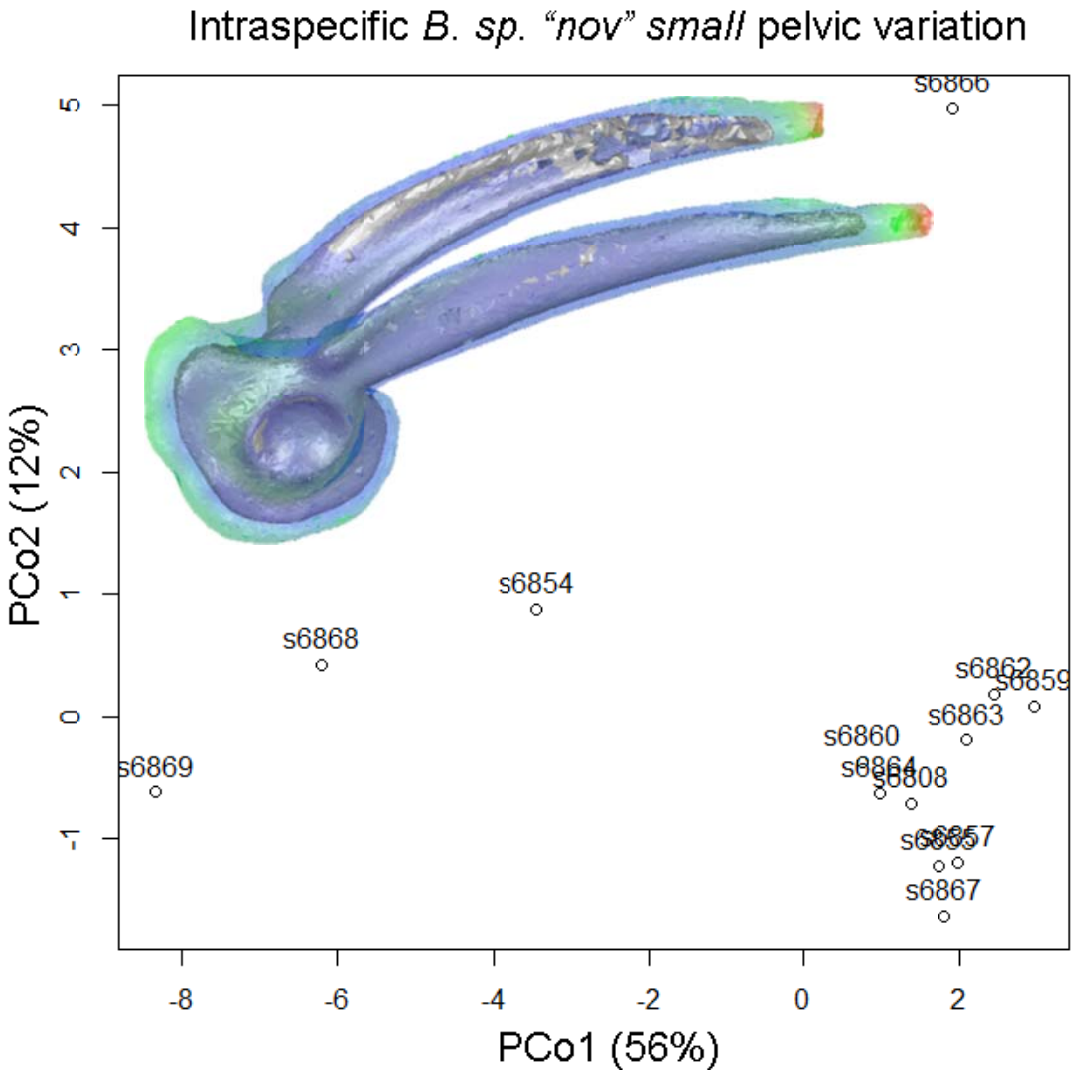

Fig. 3. Principal Coordinate PCo1 – PCo2 plot for *B. sp1 small* intraspecific pelvic shape variation standardized for size (CS = 1). Pelvic shape variation associated to PCo1 is illustrated overlaying the pelvic models described by the most negative (grey) and the most positive PCo1 scores (transparent colored) in the lateral view.

Interspecific

PCoA on the pelvic shape variation between Comorian sister species resulted in a significant species' ordination in shape space when including size variation (Wilk's $\lambda = 0$; $p = 0.050$). This is reflected on PCo1 ($p < 0.001$) for which *B. sp1 small* presents more negative values and *B. sp2 big* more positive values (Fig. 4).

Shape variation associated with increasing PCo1 value (Fig. 4) consists in a relatively increased width of the pelvis at the level of the iliac processes that results in a relatively increased lateral aperture of the iliac shafts, a relative increase in length of the iliac shafts, a relative increase in the angle of inclination of the iliac crests, and an extensive isometric

increase in size and robustness of the iliac processes, acetabulum, and entire acetabular portion of the pelvis.

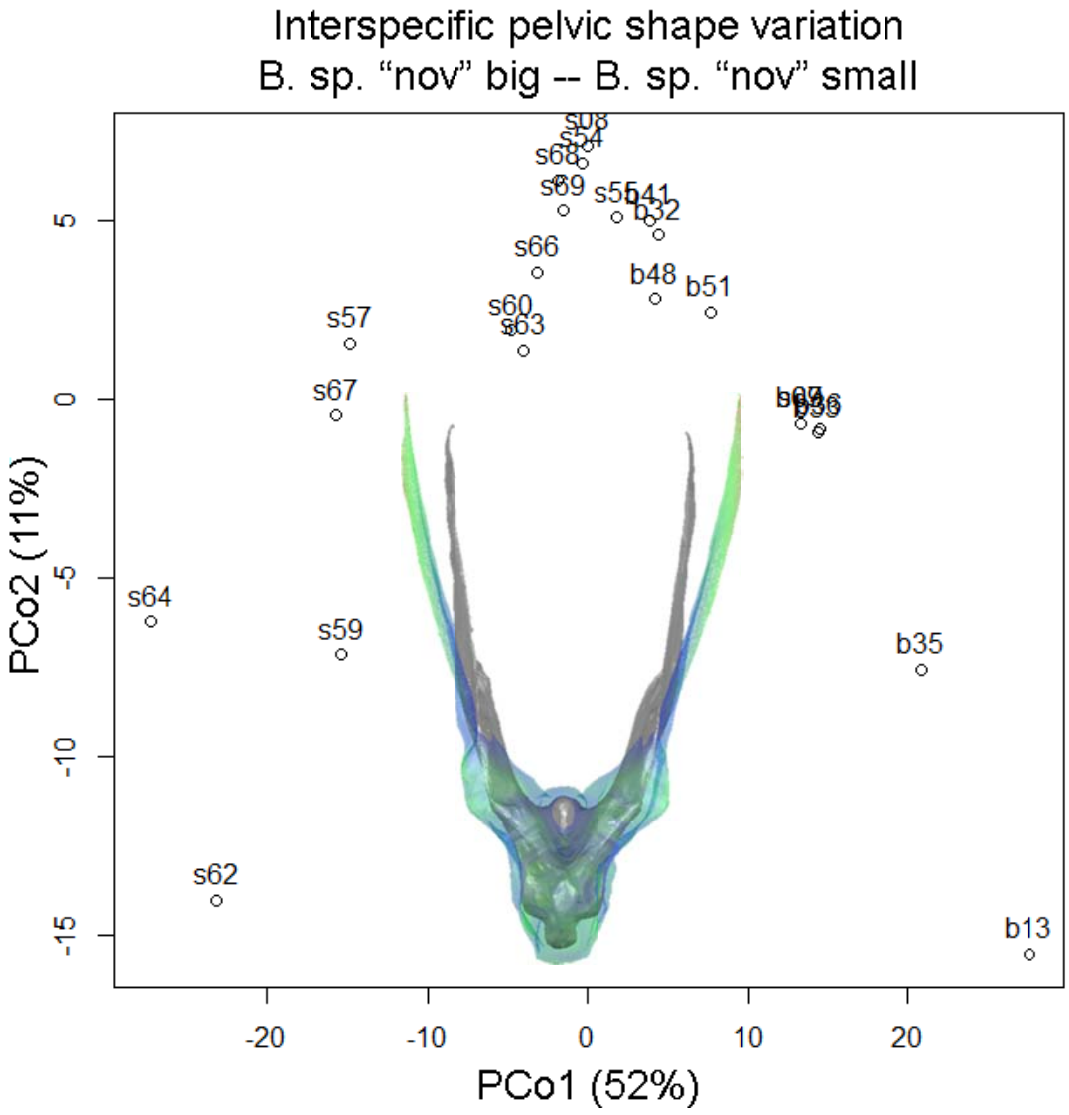

Fig. 4. Principal Coordinate PCo1 – PCo2 plot for *B. sp2 big – B. sp1 small* interspecific pelvic shape variation when including size. Pelvic shape variation associated to PCo1 is illustrated overlaying the pelvic models described by the most negative (grey) and the most positive PCo1 scores (transparent colored) in the dorsal view.

PCoA on the pelvic shape variation between the Comorian sister species and their *B. wittei* sister taxon resulted in a marginally significant species' ordination in shape space when individuals were standardized for size (Pillai's Trace = 1.992, p = 0.007; Wilk's λ = 0, p = 0.069), however this outcome was better distinguished when including size variation in the analysis (Wilk's λ = 0; p = 0.007). To focalize biologically-relevant pelvic shape variation PCoA was repeated for the three species sample utilizing as models the species' mean pelvic shape (Fig. 5).

Shape variation associated with increasing PCo1 value (Fig. 5) consists in a relative decrease in iliac shaft length, a relative increase in height of the anterior iliac crest, a relative increase in aperture of the iliac shafts, a relative decrease in height of the posterior iliac shafts, a relative decrease in robustness of the iliac processes, the acetabulum, the ventral region of the pelvis at the pubis-ischium union, the lateral surface of the ischium and the anterior ilium base, a relative increase in length along the anterior-posterior axis of the ilium base, and a relative increase in robustness of the anterior region of the pubis, of the posterior ilium base, posterior ischium margin and at the insertion of the mm. quadratus femoris and dorsal head of the adductor magnus.

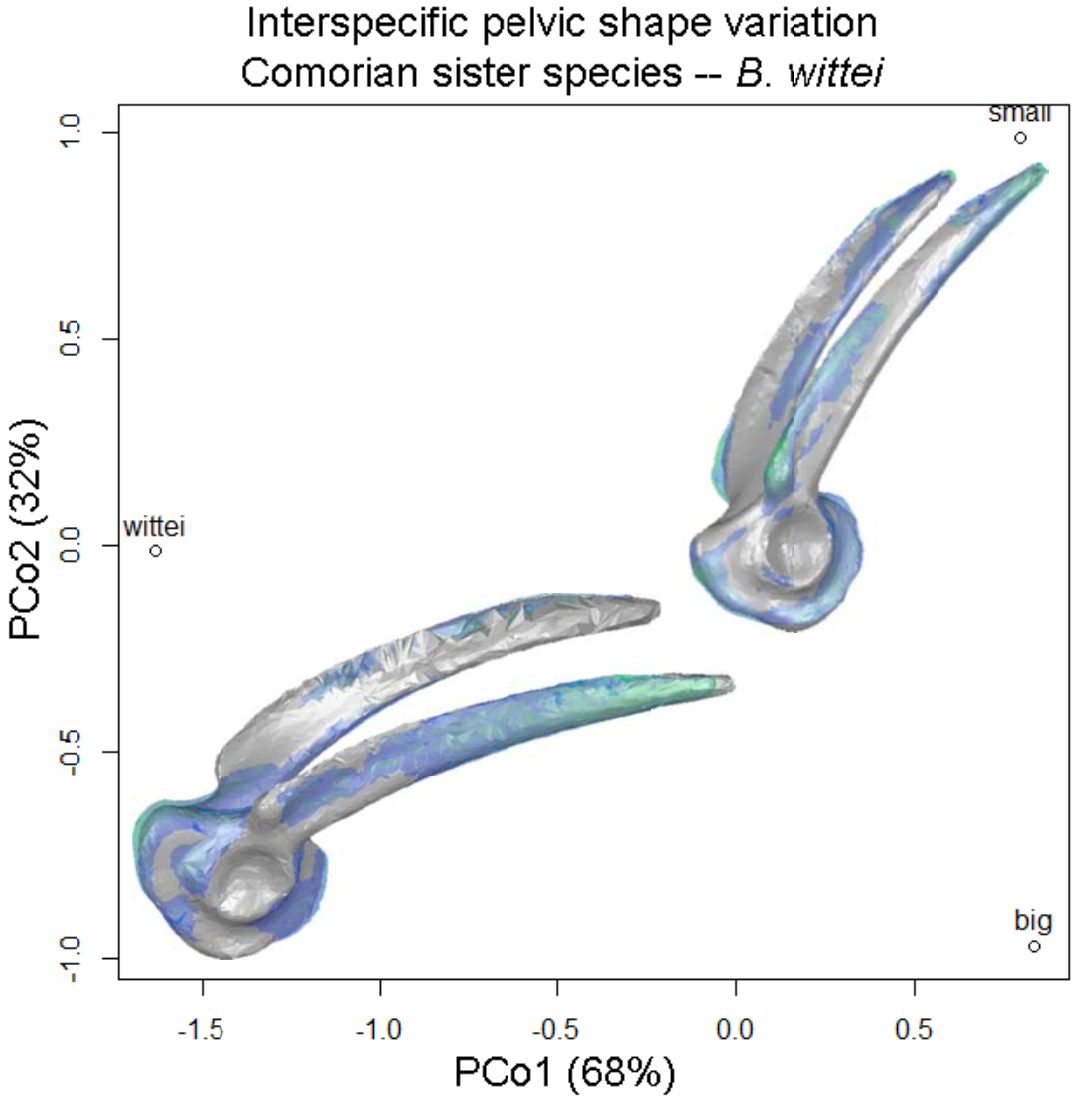

Fig. 5. Principal Coordinate PCo1 – PCo2 plot for the Comorian sister species – *B.wittei* interspecific mean pelvic shape variation standardized for size (CS = 1). Pelvic shape variation associated to PCo1 is illustrated in the bottom left corner overlaying the pelvic models described by the most negative (grey) and the most positive PCo1 scores (transparent colored) in the lateral view. Pelvic shape variation associated to PCo2 is illustrated on the right overlaying the pelvic models described by the most positive (grey) and the most negative (transparent colored) PCo2 scores in a vertical-lateral view.

Shape variation associated with decreasing PCo2 value (Fig. 5) consists in a relative increase in iliac shaft length, a relative increase in the angle of inclination of the iliac crests, a relative increase in size, height and lateral robustness of the iliac processes, and a relative increase in robustness of the anterior ilium base, anterior margin of the pubis, posterior margin of the ischium and at the insertion of the m. obturator externus.

Within-genus

PCoA on the pelvic shape variation between the seven *Blommersia* species resulted in a significant species' ordination in shape space both when standardized for size (Wilk's $\lambda = 0$, $p = 0.001$) and when including size variation (Wilk's $\lambda = 0$, $p < 0.001$). Again, PCoA was repeated for the sample utilizing as models the species' mean pelvic shape to focalize biologically-relevant pelvic shape variation (Fig. 6).

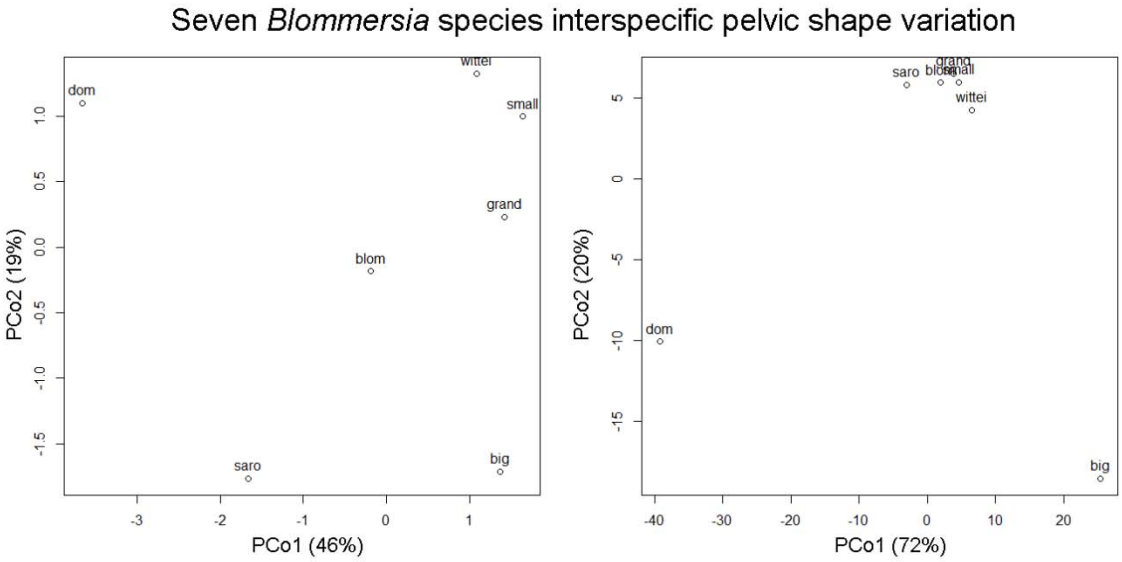

Fig. 6. Principal Coordinate PCo1 – PCo2 plot for the interspecific mean pelvic shape variation within the seven *Blommersia* species sample. Left: standardized for size (CS = 1). Right: including size variation.

Shape variation associated with increasing PCo1 values (Fig. 6 Left) consists in a relative decrease in iliac shaft length, a relative large increase in the angle of inclination of the iliac crests, a relative increase in lateral aperture of the iliac shafts starting from their posterior base, a relative increase in length along the anterior-posterior axis of the ilium base, and a relative large increase in robustness of the entire ilium base (more so anteriorly), anterior pubis, ventral pubic margin and posterior ischium margin.

Shape variation associated with decreasing PCo2 values (Fig. 6 Left) consists in a relative decrease in iliac shaft length, iliac crest height and iliac shaft aperture, a relative increase in pelvic width at the level of the iliac processes, a relative decrease in robustness of the posterior ilium base and especially of the ventral region of the pelvis at the pubis-ischium union, and a relative increase in robustness of the anterior ilium base, anterior pubic margin and ventrolateral pubic surface.

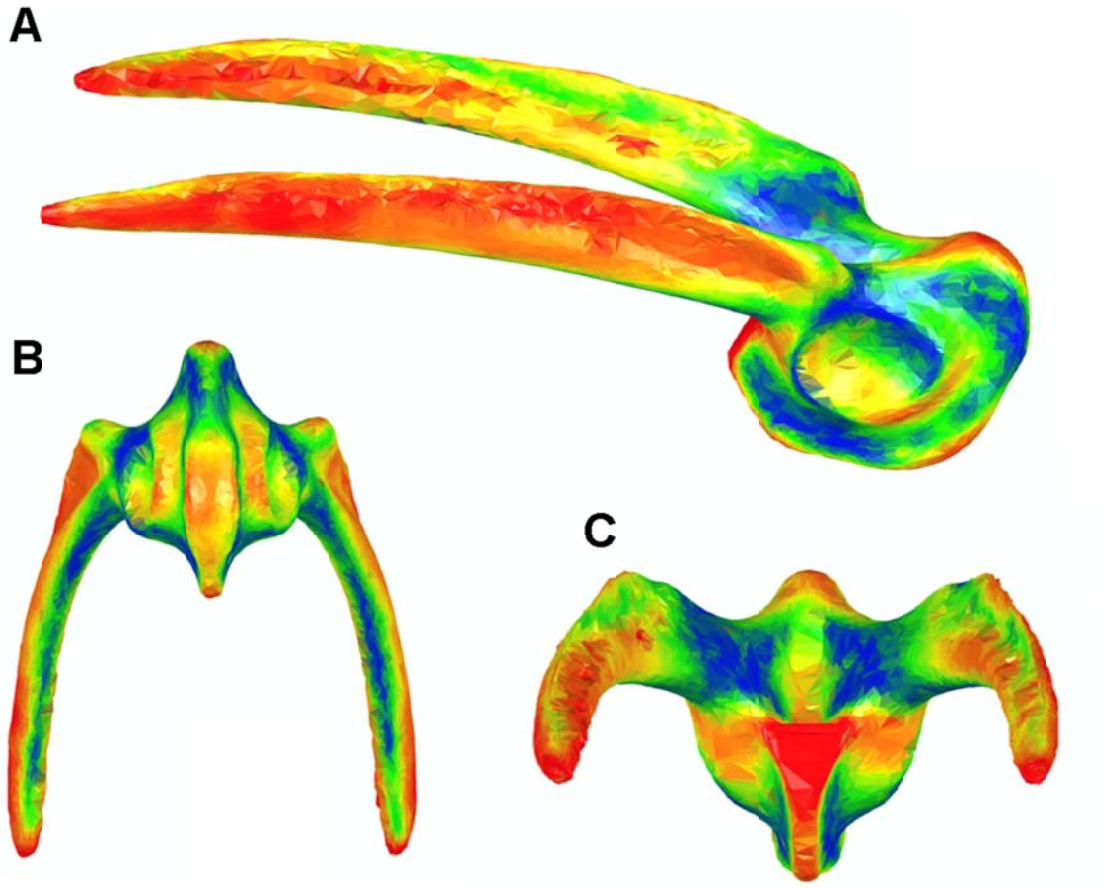

Fig. 7. Morphological disparity heatmap representation for the interspecific mean pelvic shape comparison between our seven *Blommersia* species. Variance in shape is displayed at each vertex of the 3D model obeying a color gradient from blue (lower values) to red (higher values). The range of variance values correspond to those found in the last row of the left column in Table 3.

Interspecific morphological disparity in mean pelvic shape for the seven *Blommersia* species sample (Fig. 7) illustrated high variation along the lateral surface of the iliac shafts and crests, the medial surface of the anterior iliac shafts, the anterior and posterior ilium base margins, the posteroventral acetabulum labrum, and the ventral margin of the epipubis. Low morphological disparity was observed along the ventral margin of the iliac shafts, the posterior medial base of the iliac shafts below the iliac processes, the dorsal

acetabulum labrum, the lateral surfaces of the posterior ischium, and the ventrolateral pubic surface.

Phylogenetic and Morphological Distance Mantel Test

The Mantel test between the mitochondrial rRNA 16S phylogenetic distance matrix and the morphological interspecimen PSM distance matrix (based on species' mean pelvic shapes) for the seven *Blommersia* species indicates a high positive correlation between the two datasets ($Z = 0.15775$; correlation = 0.77558; $t = 4.75825$; $\alpha=0.01$; two-tailed $p = 0.00000$). The results of 999 permutations also support this relationship (two-tailed $p = 0.001$).

DISCUSSION

Blommersia Pelvic Musculature Architecture

This is the first time that muscle insertion areas have been located and identified in a *Blommersia* species. Compared to similar previous studies in other anuran species (Duellman & Trueb, 1994; Prikryl et al., 2009) that have dissected the animals for this task, and in the process destroyed the sample for future analysis, we have been able to map the exact location of pelvic muscle insertions onto their corresponding skeletal morphology on the same individual (Fig. 2) preserving the sample for museum conservation. This has been possible thanks to the combination of CT and the application of a customized sequential two-contrast agent soft-tissue staining technique (see Materials & Methods). However, unlike these previous studies that electrically stimulated dissected muscles to determine their precise biomechanical movement, we could not evaluate the movements of the muscles in our species without destruction of the samples. Consequently, we have used their information on *Rana esculenta* as an approximation of these movements for our species due to the phylogenetic proximity of this genus to *Blommersia* (Table 2).

Comorian Pelvic Shape Evolutionary Divergence

Our analyses of intraspecific pelvic shape disparity showed an interesting pattern between the two Comorian *Blommersia* sister species and their Malagasy sister taxon. When size

variation was included for pelvic shape comparison *B. wittei* was the most variable, however when standardized for size *B. sp1 small* was the most variable (Table 3). This indicates that the potential range of size variation observed in both Comorian species may have already been present in their most recent common ancestor, and that each Comorian species has diverged on the island to opposing extremities of the size range of their Malagasy sister taxon; an outcome supported by their significantly different centroid sizes. The higher intraspecific disparity observed in the smaller Comorian species when standardized for size coincides with the tendency to miniaturization in the genus and suggests that the species is still undergoing morphological changes to adjust to smaller sizes. This observation is further reinforced by the fact that we observed sexual dimorphism in *B. sp1 small* pelvic shape consisting in a tendency towards an overall smaller and less robust pelvis in females (Fig. 3). What is more contrasting, however, is the opposite process of gigantism in *B. sp2 big* Although presenting less disparity in shape than *B. wittei*, *B. sp2 big* presented larger PSM values to its consensus, doubling those of its Malagasy sister taxon when including size variation. This indicates that this species is increasing almost isometrically in size without large changes in the species' general pelvic shape. Therefore, we can conjecture that there are less systemic morphological constraints on pelvic shape with increasing size, relative to reducing its size, in relation to pelvic locomotor function. This supposition, however, would have to be tested biomechanically and can be a topic for future research.

Interspecific comparisons of pelvic shape variation between the three species were consistent across size-standardized and non-standardized analyses, and reflected their size and phylogenetic relationships, respectively, the largest disparity in shape was between *B. sp2 big* and *B. wittei*, and the smallest between the two Comorian sister species (Table 3). However, significant patterns in pelvic shape variation between the Comorian sister species were only observed when including size variation in the analysis. Thus, we can ascertain that Comorian species present divergent size-related pelvic shape variation, but similar patterns of size-unrelated pelvic shape variation. This is reflected in the ordination of interspecific pelvic shape variation between them along PCo1 (size-related differences) and PCo2 (same pattern of size-unrelated variation) axes, respectively (Fig. 4). Pelvic shape divergence between them consisted in an isometric variation in size of the acetabular portion of the pelvis, a change in length of the iliac shafts, a change in inclination angle of the iliac crest, and in an alteration of the width of the pelvis at the

level of the iliac processes that results in a modification of the aperture between iliac shafts. Interestingly, these shape changes coincided to a large extent with those described by the PCo2 axis resulting from the ordination of the size-standardized shape variation between the three species' mean pelvic shapes (Fig. 5). Comorian sister species lie on opposite extremes of this axis of shape variation and *B. wittei* exactly in-between. Consequently, this analysis uncovers an axis of size-unrelated morphological change in pelvic shape along which the Comorian species have diverged in opposite directions from their Malagasy sister taxon. Pelvic shape variation described by this axes (PCo2, Fig. 5) differs to that described by size-related variation between Comorian species (PCo1, Fig. 4) in that the acetabular portion of the pelvis does not change isometrically, but relatively increases its robustness more towards its anterior region in *B. sp2 big* and more towards its posterior region in *B. sp2 small.* This is suggestive that development of the posterior portion of the acetabular pelvis may be more essential for conserving locomotor function during processes of miniaturization in this genus, but again, this supposition would have to be evaluated further to determine whether this is due to biomechanical and/or developmental constraints.

Both Comorian species further diverged from their sister taxon in Madagascar along an additional axis of size-unrelated pelvic shape variation (PCo1, Fig. 5). Shape changes related to the Comorian species consisted in *i)* a relative decrease in iliac shaft length accompanied by a relative increase in their lateral aperture and a variation in their height, which increases anteriorly, but decreases posteriorly, *ii)* relatively smaller iliac processes, but displaying a relatively increased length of the ilium base along its anterior-posterior axis, and *iii)* a relatively more robust lateral surface of the dorsal pubis and dorsal margin of the ischium. Apparently all these observed changes in pelvic shape may affect associated muscle architecture, and ultimately jumping locomotor performance, and will be discussed below in the context of the evolution of the anuran musculoskeletal locomotor system.

Blommersia Phylogenetic Pelvic Shape Evolution

The aforementioned axis of pelvic shape variation between Comorian sister species and their Malagasy sister taxon (PCo1, Fig. 5) coincides to a large extent with that observed between the mean pelvic shapes of the seven *Blommersia* species included in this study

(PCo1, Fig. 6 Left), albeit with slight differences on the acetabular portion of the pelvis, and may represent a major axis of pelvic shape variation in the genus. Interestingly, morphological changes along the PCo2 axis of the *Blommersia* interspecific pelvic shape analysis (PCo2, Fig. 6) also coincide to a large extent with those discriminating Comorian sister species (PCo1, Fig. 5), potentially representing an additional major axis of pelvic shape variation within the genus. We can confirm that these axes describe relevant patterns for species' pelvic shape divergence within our small subsample of the *Blommersia* genus given the high correlation (0.77; p = 0.001) observed between our species' morphological and genetic distance matrices. However, whether or not these patterns are phylogenetically widespread within the genus should be corroborated in the future with further analyses including the pelvic shapes of additional *Blommersia* species.

In the size-standardized PCo1-PCo2 morphospace (Fig. 6 Left) we observe several patterns of pelvic shape divergence that reflect the phylogenetic relationships between our *Blommersia* species. First of all, the oldest species pair (*B. sarotra – B. grandisonae*, Fig. 1) is the only one to cover the complete range of shape variation of the biplot (*i.e.* positive and negative values on both axes; first and third quadrants) potentially indicating a longer time for divergence, and the more recent *B. domerguei – B. blommersae* species pair essentially occupies the second quadrant (*i.e.* negative PCo1, positive PCo2 values) consequently not overlapping in morphospace with the preceding species pair. In the same manner, the *B. wittei – B. sp1 small* species pair covers the region of the first quadrant unoccupied by previous species pairs, however *B. sp2 big* diverges greatly from the position of *B. wittei* and its Comorian sister species in the shared morphospace and is the only species that occupies the fourth quadrant. The great leap of *B. sp2 big* into an unoccupied area of the shared morphospace so far away from its phylogenetically closest relatives, and jumping over the position of *B. grandisonae*, advocates that it has potentially undergone a process of 'morphological release' on Mayotte by occupying part of the morphospace that is likely filled by other, larger anuran species from mainland Madagascar.

Evolution of the Blommersia Musculoskeletal Locomotor System

The morphological disparity in pelvic shape observed between the seven analyzed *Blommersia* species was largely concentrated on the lateral and medial iliac shafts and on

the anterior and posterior ilium base (red, Fig. 7). These morphological structures constitute anatomical regions that are highly derived in anurans relative to their tetrapod ancestors and that have favored the evolution of different types of locomotion (Prikryl et al., 2009). The reabsorption of the pubis and anterior expansion of the iliac shafts, simultaneously with the reduction of the tail into an urostyle, have promoted the continuous diversification of the musculature associated to these structures to adapt to diverse locomotor requirements (Gans & Parsons, 1966). This has resulted in modifications of the musculature inserting on the iliac shaft and ilium base (*i.e.* no. 1-3, 7-9; Fig. & Table 2) involved in the anterior movement of the femur and responsible for the crouching position of anurans that allows them to generate relatively large forces in short timespans (Burkholder & Lieber, 2001; Gillis, 2010; Reilly et al., 2016). Conversely, the musculature involved in thrust production (*i.e.* no. 4-6, 10, 12-13, 17, 19, 23; Fig. & Table 2) have been modified the least relative to their ancestral positions on the pelvis (Prikryl et al., 2009). Accordingly, these muscles insert on the pelvic regions of less disparity between these *Blommersia* species (blue, Fig. 7). However, in specialized terrestrial jumpers, as the majority of mantellids including the *Blommersia* genus (Reilly & Jorgensen, 2011), these muscles have become relatively larger and more diversified than in other anurans exhibiting dissimilar locomotor modes, consequently increasing absolute force production during jumping (Zug, 1978; James et al., 2007). Therefore the variation in length along the anterior-posterior axis of the ilium base we observe between our *Blommersia* species may correspond to an isometric variation in size modifying the available space below for the insertion of these muscles. In addition, while the pelvic shape disparity observed within our *Blommersia* species sample largely corresponds to the general pattern of pelvic musculature evolution from tetrapods to anurans, we observed relatively large amounts of disparity at the iliac process (yellow-green, Fig. 7). Given the stable evolutionary origin (Prikryl et al., 2009) of the musculature on this structure (no. 4-6, Fig. 7), we believe that the disparity in pelvic shape at this structure may be due more to size differentiation between *Blommersia* species than to correlation with muscular insertion.

The axes of shape variation describing significant interspecific differences in pelvic shape between the studied *Blommersia* species (see above) point to more specific differences in morphology that may be potentially implicated in their ecological diversification and correlated to a species' lifestyle, habitat use, and locomotor performance (Gomes et al.,

2009). With this in mind we hypothesize that the ecological pressures associated to the colonization of novel environments during the *Blommersia* species' divergence would have determined the development of pelvic shape through its morphofunctional association with locomotor performance. In mantellids, miniaturization parallels species diversity (Wollenberg et al., 2011). Smaller body sizes are believed to limit species' dispersal capabilities, resulting in smaller and more fragmented geographic ranges that potentially facilitate reproductive isolation and ultimately speciation. However, a smaller body size also reduces physiological tolerances and does not permit the colonization of novel areas due to limited dispersal capabilities, causing an opposite effect on the speciation process (Pabijan et al., 2012). The shape variation associated to 'miniaturization/gigantism' in our Comorian species relative to their Malagasy sister taxon were largely determined by isometric size differences in the iliac shafts' length, aperture, and width between the iliac processes (Figs. 3 & 4); the only size-unrelated variation consisting in a more developed anterior region of the acetabular region in the larger species relative to its posterior region in the smaller one (PCo2, Fig. 5). If we consider the shape variation associated to the isometric increase in size to result in a linear increase in locomotor performance (*e.g.* in jump distance; Emerson, 1978, but see James et al., 2007), this difference between the Comorian species advocates a trade-off between thigh extension and flexion during locomotion [with reference to the locomotor function of the predominant muscles inserting on these areas (no. 10 & 19, Table 2)] that may be correlated to their differential preferred habitat and lifestyle. However, to corroborate this hypothesis a reciprocal transplant experiment testing their biomechanical locomotor performance in the different environments would be necessary. Additional analogous experiments between other *Blommersia* species may as well be considered to evaluate whether the observed pelvic morphological differences correlate to contrasting locomotor performance within different habitats.

ACKNOWLEDGEMENTS

We would like to thank the members of the University of Antananarivo, Department of Animal Biology for giving us access to their museum collections, and to Christina Paradela from the internal Service of Non-destructive Techniques (MNCN-CSIC) for the hours spent CT-scanning our own specimens. This research was funded by the Spanish Ministry of Economy and Competitiveness; grant number CGL2013-40924-P.

REFERENCES

Besl PJ, McKay ND (1992) Method for registration of 3-D shapes. In *Sensor Fusion IV: Control Paradigms and Data Structures*), pp. 586-607. International Society for Optics and Photonics.

Burkholder TJ, Lieber RL (2001) Sarcomere length operating range of vertebrate muscles during movement. *Journal of Experimental Biology,* **204,** 1529-1536.

Chen Y, Medioni G (1992) Object modelling by registration of multiple range images. *Image and Vision Computing,* **10,** 145-155.

Cignoni P, Callieri M, Corsini M, Dellepiane M, Ganovelli F, Ranzuglia G (2008) Meshlab: an open-source mesh processing tool. In *Eurographics Italian Conference*), pp. 129-136.

Descamps E, Sochacka A, De Kegel B, Van Loo D, Van Hoorebeke L, Adriaens D (2014) Soft tissue discrimination with contrast agents using micro-CT scanning. *Belgian Journal of Zoology,* **144,** 20-40.

Duellman WE, Trueb L (1994) *Biology of Amphibians,* JHU Press.

Duncan R, Turner C (1995) Mechanotransduction and the functional response of bone to mechanical strain. *Calcified Tissue International,* **57,** 344-358.

Emerson SB (1978) Allometry and jumping in frogs: helping the twain to meet. *Evolution,* **32,** 551-564.

Emerson SB (1982) Frog postcranial morphology: identification of a functional complex. *Copeia,* **1982,** 603-613.

Emerson SB, De Jongh H (1980) Muscle activity at the ilio-sacral articulation of frogs. *Journal of Morphology,* **166,** 129-144.

Essner RL, Suffian DJ, Bishop PJ, Reilly SM (2010) Landing in basal frogs: evidence of saltational patterns in the evolution of anuran locomotion. *Naturwissenschaften,* **97,** 935-939.

Gans C, Parsons TS (1966) On the origin of the jumping mechanism in frogs. *Evolution,* **20,** 92-99.

Gignac PM, Kley NJ (2014) Iodine-enhanced micro-CT imaging: methodological refinements for the study of the soft-tissue anatomy of post-embryonic vertebrates. *Journal of Experimental Zoology Part B: Molecular and Developmental Evolution,* **322,** 166-176.

Gillis GB (2010) Frog muscles start stretched. *Journal of Experimental Biology,* **213,** vi-vi.

Gomes F, Rezende E, Grizante M, Navas C (2009) The evolution of jumping performance in anurans: morphological correlates and ecological implications. *Journal of Evolutionary Biology,* **22,** 1088-1097.

Handrigan GR, Wassersug RJ (2007) The anuran Bauplan: a review of the adaptive, developmental, and genetic underpinnings of frog and tadpole morphology. *Biological Reviews,* **82,** 1-25.

Hudson CM, Brown GP, Shine R (2016) Athletic anurans: the impact of morphology, ecology and evolution on climbing ability in invasive cane toads. *Biological Journal of the Linnean Society,* **119,** 992-999.

James RS, Navas CA, Herrel A (2007) How important are skeletal muscle mechanics in setting limits on jumping performance? *Journal of Experimental Biology,* **210,** 923-933.

Lires AI, Soto IM, Gómez RO (2016) Walk before you jump: new insights on early frog locomotion from the oldest known salientian. *Paleobiology,* **42,** 612-623.

Pabijan M, Wollenberg K, Vences M (2012) Small body size increases the regional differentiation of populations of tropical mantellid frogs (Anura: Mantellidae). *Journal of Evolutionary Biology,* **25,** 2310-2324.

Pomidor BJ, Makedonska J, Slice DE (2016) A landmark-free method for three-dimensional shape analysis. *PLoS One,* **11,** e0150368.

Přikryl T, Aerts P, Havelková P, Herrel A, Roček Z (2009) Pelvic and thigh musculature in frogs (Anura) and origin of anuran jumping locomotion. *Journal of Anatomy,* **214,** 100-139.

Reilly SM, Jorgensen ME (2011) The evolution of jumping in frogs: morphological evidence for the basal anuran locomotor condition and the radiation of locomotor systems in crown group anurans. *Journal of Morphology,* **272,** 149-168.

Reilly SM, Montuelle SJ, Schmidt A, Krause C, Naylor E, Jorgensen ME, Essner Jr RL (2016) Pelvic function in anuran jumping: interspecific differences in the kinematics and motor control of the iliosacral articulation during take-off and landing. *Journal of Morphology,* **277,** 1539-1558.

Rohlf FJ, Slice D (1990) Extensions of the Procrustes method for the optimal superimposition of landmarks. *Systematic Biology,* **39,** 40-59.

Scherz MD, Hawlitschek O, Andreone F, Rakotoarison A, Vences M, Glaw F (2017a) A review of the taxonomy and osteology of the *Rhombophryne serratopalpebrosa* species group (Anura: Microhylidae) from Madagascar, with comments on the value of volume rendering of micro-CT data to taxonomists. *Zootaxa,* **4273,** 301-340.

Scherz MD, Razafindraibe JH, Rakotoarison A, Dixit NM, Bletz MC, Glaw FR, Vences M (2017b) Yet another small brown frog from high altitude on the Marojejy Massif, northeastern Madagascar (Anura: Mantellidae). *Zootaxa,* **4347,** 572-582.

Sigurdsen T, Green DM, Bishop PJ (2012) Did Triadobatrachus jump? Morphology and evolution of the anuran forelimb in relation to locomotion in early salientians. *Fieldiana Life and Earth Sciences,* ***2012,*** 77-89.

Tamura K, Nei M, Kumar S (2004) Prospects for inferring very large phylogenies by using the neighbor-joining method. *Proceedings of the National Academy of Sciences,* **101,** 11030-11035.

Tamura K, Stecher G, Peterson D, Filipski A, Kumar S (2013) MEGA6: molecular evolutionary genetics analysis version 6.0. *Molecular Biology and Evolution,* **30,** 2725-2729.

Vickerton P, Jarvis J, Jeffery N (2013) Concentration-dependent specimen shrinkage in iodine-enhanced micro CT. *Journal of Anatomy,* **223,** 185-193.

Vieites DR, Wollenberg KC, Andreone F, Köhler J, Glaw F, Vences M (2009) Vast underestimation of Madagascar's biodiversity evidenced by an integrative amphibian inventory. *Proceedings of the National Academy of Sciences,* **106,** 8267-8272.

Wainwright PC, Alfaro ME, Bolnick DI, Hulsey CD (2005) Many-to-one mapping of form to function: a general principle in organismal design? *Integrative and Comparative Biology,* **45,** 256-262.

Whittaker RJ, Fernández-Palacios JM (2007) *Island Biogeography: ecology, evolution, and conservation,* Oxford University Press.

Wollenberg KC, Vieites DR, Glaw F, Vences M (2011) Speciation in little: the role of range and body size in the diversification of Malagasy mantellid frogs. *BMC Evolutionary Biology,* **11,** 217.

Zug GR (1978) Anuran Locomotion—Structure and Function, 2: Jumping Performance of Semiaquatic, Terrestrial, and Arboreal Frogs. *Smithsonian Contributions to Zoology,* **276**.

SUPPLEMENTARY MATERIAL

Table S1. Holding collection, field number, sex, and locality of recollection of the Comorian *Blommersia* individuals that were stained to enhance muscle visualization.

Species	Collection	Field no.	Sex	Locality
B. sp2 big	MNCN	DRV6834	M	Mont Benara
	MNCN	DRV6837	M	Mont Benara
	MNCN	DRV6840	M	Mont Benara
	MNCN	DRV6851	F	Mont Combani
B. sp1 small	MNCN	DRV6809	F	Mont Sapere
	MNCN	DRV6856	M	Mont Sapere
	MNCN	DRV6864	M	Mont Sapere
	MNCN	DRV6866	M	Mont Sapere

Videos S1 & S2. Video along the 2D sagittal plane of contrast stained specimen DRV6834 *B. sp2 big* illustrating the musculature associated to the pelvis and urostyle [grey values: 12000-55500; greyscale (S1) and seismic (S2) colormaps]. The initial and final positions of the video are shown in Fig. S1. The position of the skeletal structures are visualized as a transparent renderization within the videos.

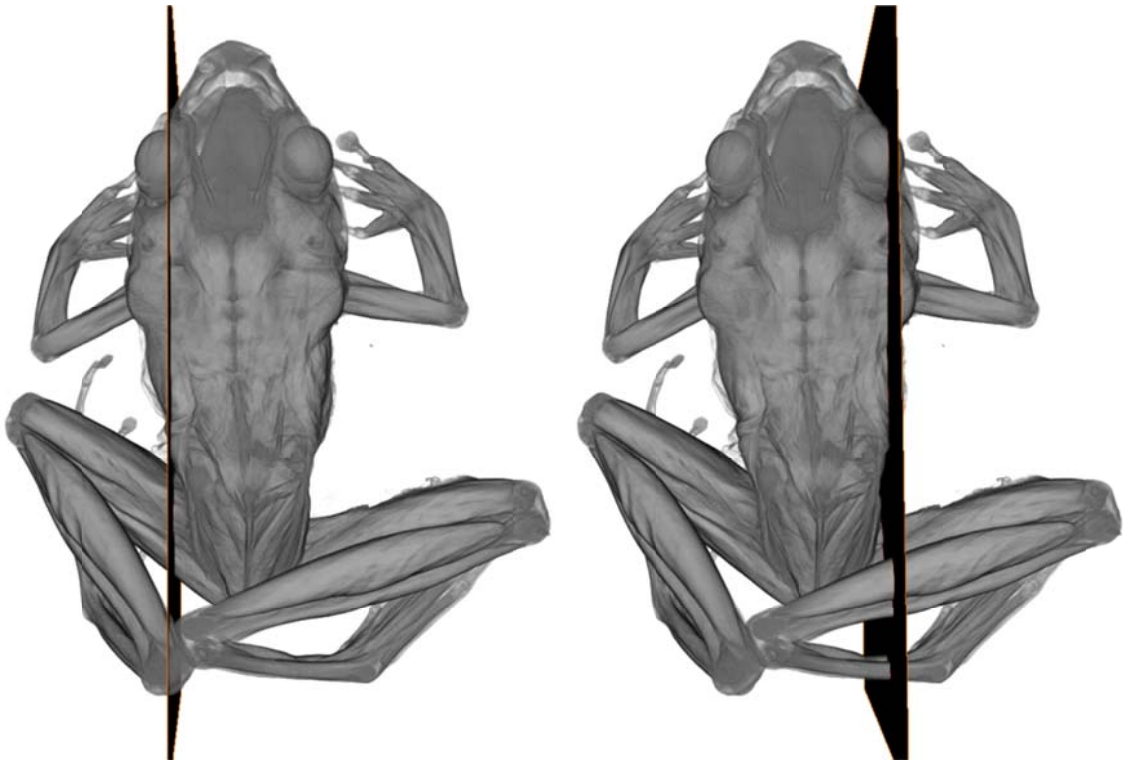

Fig. S1. Cutting planes along the sagittal axis corresponding to the visualization of Videos S1 & S2.

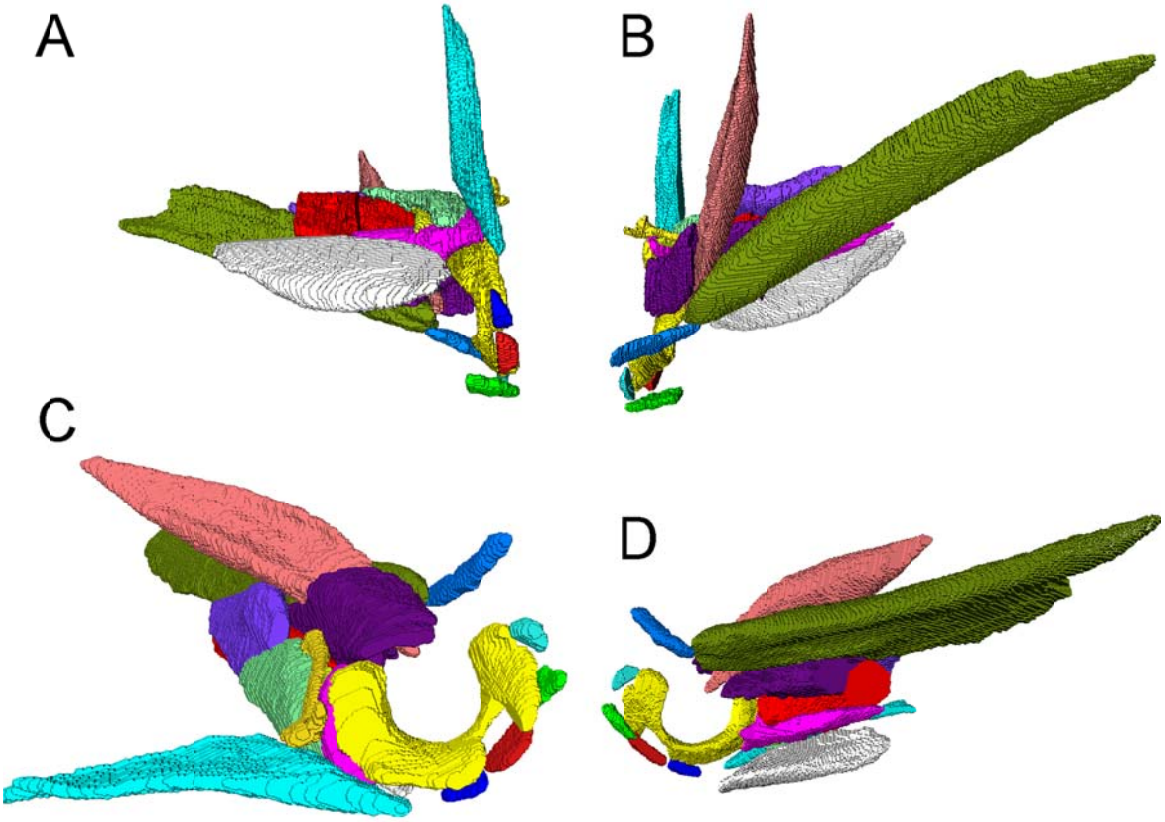

Fig. S2. Images of the ongoing segmentation of the pelvic musculature of *B. sp2 big*. **A:** ventral view. **B:** dorsal view. **C:** medial sagittal view. **D:** lateral sagittal view. Images correspond to the right leg of specimen DRV6834.